AD

Technical Report ARAEW-TR-04002

MODELING OF TRANSIENT THERMAL DAMAGE IN CERAMICS FOR CANNON BORE APPLICATIONS

J.H. Underwood, M.E. Todaro, G.N. Vigilante

MARCH 2004

ARMAMENT RESEARCH, DEVELOPMENT AND ENGINEERING CENTER
Armaments Engineering & Technology Center
Weapon Systems & Technology
Benét Laboratories
Watervliet, New York

APPROVED FOR PUBLIC RELEASE; DISTRIBUTION UNLIMITED

Report Documentation Page

Form Approved
OMB No. 0704-0188

1. REPORT DATE	2. REPORT TYPE	3. DATES COVERED
MAR 2004	**FINAL**	**00-00-2002 to 00-00-2003**

4. TITLE AND SUBTITLE
MODELING OF TRANSIENT THERMAL DAMAGE IN CERAMICS

5a. CONTRACT NUMBER
5b. GRANT NUMBER
5c. PROGRAM ELEMENT NUMBER

6. AUTHOR(S)
John Underwood; Mark Todaro; Gregory Vigilante

5d. PROJECT NUMBER
5e. TASK NUMBER
5f. WORK UNIT NUMBER

7. PERFORMING ORGANIZATION NAME(S) AND ADDRESS(ES)
U.S. ARMY ARDEC,Benet Laboratories, RDAR-WSB,Watervliet,NY,12198

8. PERFORMING ORGANIZATION REPORT NUMBER
ARAEW-TR-04002

9. SPONSORING/MONITORING AGENCY NAME(S) AND ADDRESS(ES)
U.S. ARMY ARDEC, Benet Laboratories, RDAR-WSB, Watervliet, NY, 12198

10. SPONSOR/MONITOR'S ACRONYM(S)

11. SPONSOR/MONITOR'S REPORT NUMBER(S)

12. DISTRIBUTION/AVAILABILITY STATEMENT
Approved for public release; distribution unlimited

13. SUPPLEMENTARY NOTES

14. ABSTRACT
Higher and more sustained cannon combustion-gas temperatures have led to interest in ceramics as a thermal barrier material at a cannon bore. Some initial work with SiC [1] showed cracks at a surface heated by a laser to similar temperature and duration as severe cannon firing. Finite difference and solid mechanics analysis of the thermal damage indicated that failure near the surface occurred when the transient thermal stress exceeded the reduced high-temperature compressive strength, leading to permanent ompressive strain and subsequent tensile residual stress and cracking upon cooling. The purpose here is to perform laser-heating tests with seven additional ceramics and to compare damage from laser heating with that predicted from modeling hot-gas heating typical of cannon firing. In this case, the finite difference calculation of transient temperature includes detailed time-varying values of cannon gas temperature and onvection coefficient, allowing a more realistic characterization of cannon thermal damage.

15. SUBJECT TERMS

16. SECURITY CLASSIFICATION OF:			17. LIMITATION OF ABSTRACT	18. NUMBER OF PAGES	19a. NAME OF RESPONSIBLE PERSON
a. REPORT	b. ABSTRACT	c. THIS PAGE			
unclassified	**unclassified**	**unclassified**	**Same as Report (SAR)**	**12**	

REPORT DOCUMENTATION PAGE

Form Approved
OMB No. 0704-0188

1. REPORT DATE *(DD-MM-YYYY)*
01-03-2004

2. REPORT TYPE
FINAL

3. DATES COVERED *(From - To)*

4. TITLE AND SUBTITLE
MODELING OF TRANSIENT THERMAL DAMAGE IN CERAMICS FOR CANNON BORE APPLICATIONS

5a. CONTRACT NUMBER

5b. GRANT NUMBER

5c. PROGRAM ELEMENT NUMBER

6. AUTHOR(S)
J.H. Underwood, M.E. Todaro, G.N. Vigilante

5d. PROJECT NUMBER

5e. TASK NUMBER

5f. WORK UNIT NUMBER

7. PERFORMING ORGANIZATION NAME(S) AND ADDRESS(ES)
U.S. Army ARDEC
Benet Laboratories, RDAR-WSB
Watervliet, NY 12189-4000

8. PERFORMING ORGANIZATION REPORT NUMBER
ARAEW-TR-04002

9. SPONSORING/MONITORING AGENCY NAME(S) AND ADDRESS(ES)
U.S. Army ARDEC
Benet Laboratories, RDAR-WSB
Watervliet, NY 12189-4000

10. SPONSOR/MONITOR'S ACRONYM(S)

11. SPONSORING/MONITORING AGENCY REPORT NUMBER

12. DISTRIBUTION AVAILABILITY STATEMENT
Approved for public release; distribution is unlimited or other distribution statement.

13. SUPPLEMENTARY NOTES

14. ABSTRACT
Higher and more sustained cannon combustion-gas temperatures have led to interest in ceramics as a thermal barrier material at a cannon bore. Some initial work with SiC [1] showed cracks at a surface heated by a laser to similar temperature and duration as severe cannon firing. Finite difference and solid mechanics analysis of the thermal damage indicated that failure near the surface occurred when the transient thermal stress exceeded the reduced high-temperature compressive strength, leading to permanent compressive strain and subsequent tensile residual stress and cracking upon cooling. The purpose here is to perform laser-heating tests with seven additional ceramics and to compare damage from laser heating with that predicted from modeling hot-gas heating typical of cannon firing. In this case, the finite difference calculation of transient temperature includes detailed time-varying values of cannon gas temperature and convection coefficient, allowing a more realistic characterization of cannon thermal damage.

15. SUBJECT TERMS

16. SECURITY CLASSIFICATION OF: a. REPORT	b. ABSTRACT	c. THIS PAGE	17. LIMITATION OF ABSTRACT	18. NUMBER OF PAGES	19a. NAME OF RESPONSIBLE PERSON
U/U	U	U	U	12	Mark E Todaro
					19b. TELEPONE NUMBER (*Include area code*) 518-266-5237

INSTRUCTIONS FOR COMPLETING SF 298

1. REPORT DATE. Full publication date, including day, month, if available. Must cite at lest the year and be Year 2000 compliant, e.g., 30-06-1998; xx-08-1998; xx-xx-1998.

2. REPORT TYPE. State the type of report, such as final, technical, interim, memorandum, master's thesis, progress, quarterly, research, special, group study, etc.

3. DATES COVERED. Indicate the time during which the work was performed and the report was written, e.g., Jun 1997 - Jun 1998; 1-10 Jun 1996; May - Nov 1998; Nov 1998.

4. TITLE. Enter title and subtitle with volume number and part number, if applicable. On classified documents, enter the title classification in parentheses.

5a. CONTRACT NUMBER. Enter all contract numbers as they appear in the report, e.g. F33615-86-C-5169.

5b. GRANT NUMBER. Enter all grant numbers as they appear in the report, e.g. 1F665702D1257.

5c. PROGRAM ELEMENT NUMBER. Enter all program element numbers as they appear in the report, e.g. AFOSR-82-1234.

5d. PROJECT NUMBER. Enter al project numbers as they appear in the report, e.g. 1F665702D1257; ILIR.

5e. TASK NUMBER. Enter all task numbers as they appear in the report, e.g. 05; RF0330201; T4112.

5f. WORK UNIT NUMBER. Enter all work unit numbers as they appear in the report, e.g. 001; AFAPL30480105.

6. AUTHOR(S). Enter name(s) of person(s) responsible for writing the report, performing the research, or credited with the content of the report. The form of entry is the last name, first name, middle initial, and additional qualifiers separated by commas, e.g. Smith, Richard, Jr.

7. PERFORMING ORGANIZATION NAME(S) AND ADDRESS(ES). Self-explanatory.

8. PERFORMING ORGANIZATION REPORT NUMBER. Enter all unique alphanumeric report numbers assigned by the performing organization, e.g. BRL-1234; AFWL-TR-85-4017-Vol-21-PT-2.

9. SPONSORING/MONITORS AGENCY NAME(S) AND ADDRESS(ES). Enter the name and address of the organization(s) financially responsible for and monitoring the work.

10. SPONSOR/MONITOR'S ACRONYM(S). Enter, if available, e.g. BRL, ARDEC, NADC.

11. SPONSOR/MONITOR'S REPORT NUMBER(S). Enter report number as assigned by the sponsoring/ monitoring agency, if available, e.g. BRL-TR-829; -215.

12. DISTRIBUTION/AVAILABILITY STATEMENT. Use agency-mandated availability statements to indicate the public availability or distribution limitations of the report. If additional limitations/restrictions or special markings are indicated, follow agency authorization procedures, e.g. RD/FRD, PROPIN, ITAR, etc. Include copyright information.

13. SUPPLEMENTARY NOTES. Enter information not included elsewhere such as: prepared in cooperation with; translation of; report supersedes; old edition number, etc.

14. ABSTRACT. A brief (approximately 200 words) factual summary of the most significant information.

15. SUBJECT TERMS. Key words or phrases identifying major concepts in the report.

16. SECURITY CLASSIFICATION. Enter security classification in accordance with security classification regulations, e.g. U, C, S, etc. If this form contains classified information, stamp classification level on the top and bottom of this page.

17. LIMITATION OF ABSTRACT. This block must be completed to assign a distribution limitation to the abstract. Enter UU (Unclassified Unlimited) or SAR (Same as Report). An entry in this block is necessary if the abstract is to be limited.

TABLE OF CONTENTS

Figures & Tables

INTRODUCTION

Higher and more sustained cannon combustion-gas temperatures have led to interest in ceramics as a thermal barrier material at a cannon bore. Some initial work with SiC [1] showed cracks at a surface heated by a laser to similar temperature and duration as severe cannon firing. Finite difference and solid mechanics analysis of the thermal damage indicated that failure near the surface occurred when the transient thermal stress exceeded the reduced high-temperature compressive strength, leading to permanent compressive strain and subsequent tensile residual stress and cracking upon cooling. The purpose here is to perform laser-heating tests with seven additional ceramics and to compare damage from laser heating with that predicted from modeling hot-gas heating typical of cannon firing. In this case, the finite difference calculation of transient temperature includes detailed time-varying values of cannon gas temperature and convection coefficient, allowing a more realistic characterization of cannon thermal damage.

CERAMIC MATERIALS AND PROPERTIES

Table I lists the seven ceramics studied, along with properties E, ? and a used in the analysis. The thermal conductivity, k, and diffusivity, d, were determined for temperatures of 300-1270 K using a laser flash method [2]. Compressive strengths over 300-1070 K were determined from elevated temperature hardness tests, using the known

Table I – Ceramics investigated and selected properties

Ceramic	**Elastic Modulus** E; GPa	**Poisson's Ratio** ? --	**Thermal Expansion** a; K^{-1}	**Thermal Conduction** k; W/m K	**Thermal Diffusivity** d; cm^2/s	**Compressive Strength** S_C; GPa
ZrO_2	210	0.23	12.E-6	$12.7\ T^{-0.247}$	$0.126\ T^{-0.434}$	$531\ T^{-0.882}$
Al_2O_3	370	0.22	8.5E-6	$9610\ T^{-1.011}$	$175\ T^{-1.324}$	$780\ T^{-0.845}$
SiAlON	320	0.25	3.3E-6	$28.3\ T^{-0.170}$	$0.714\ T^{-0.503}$	$35.0\ T^{-0.283}$
Si_3N_4	310	0.27	3.2E-6	$339\ T^{-0.442}$	$14.1\ T^{-0.844}$	$33.3\ T^{-0.324}$
SiC-2	410	0.14	4.8E-6	$2000\ T^{-0.567}$	$64.8\ T^{-0.927}$	$182\ T^{-0.569}$
SiC-1	430	0.17	4.9E-6	$5240\ T^{-0.687}$	$218\ T^{-1.086}$	$226\ T^{-0.590}$
SiC-3	410	0.14	4.5E-6	$33600\ T^{-0.922}$	$1110\ T^{-1.287}$	$445\ T^{-0.665}$

relationship [3] that compressive strength, S_C , is well approximated as one third of hardness. Vickers hardness, HV, was used in the tests here in units of kg/mm^2. The resulting expression for S_C in units of GPa is:

$$S_C = (1/3)\ HV \bullet 0.0098\ GPa/(kg/mm^2) \quad (1)$$

Power-law expressions were fitted to the k, d and S_C data at room and elevated temperature, as shown in Table I for each of the seven ceramics and in the example plots of Figure 1 for Si_3N_4. The power law fits well and remains positive at high temperature, a requirement for thermal-mechanical modeling.

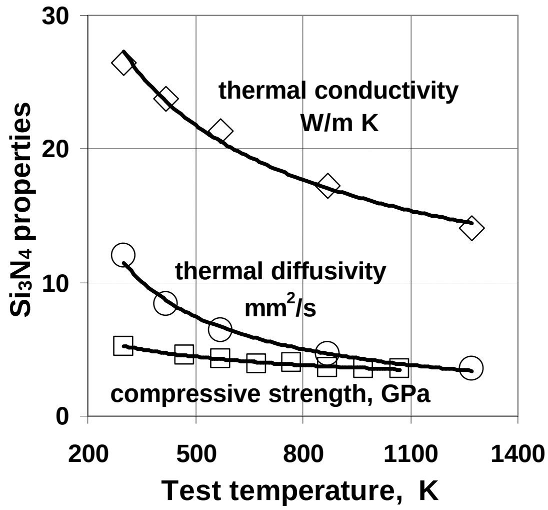

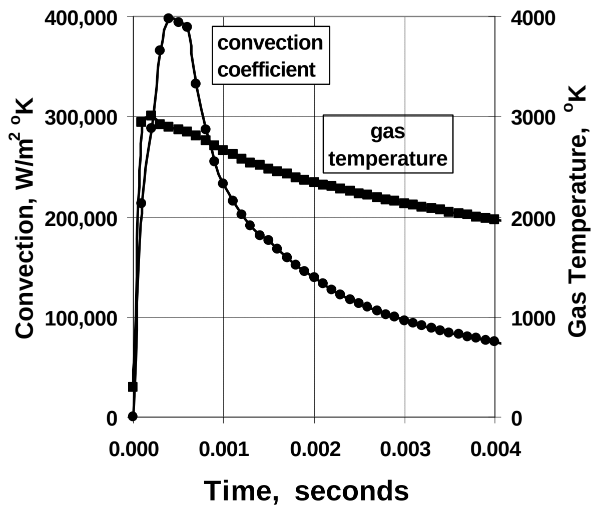

Figure 1. Example model input data for Si_3N_4

Figure 2. Hot gas input data for cannon firing

THERMO-MECHANICAL MODELING

Modeling of the transient temperatures and associated thermal damage at a cannon bore is similar to that in prior work [1,4], but with two improvements, summarized in Figures 1 and 2. First, the current modeling incorporates compressive strength vs temperature (Figure 1), gleaned from hot hardness measurements over a range of temperature for each of the seven ceramics. Prior work used literature values of hardness for generally similar materials. Second, the current model also incorporates detailed time-varying cannon combustion gas temperature and convection coefficient data (Figure 2) in the finite difference calculation of the near-bore temperature distribution. The hot gas data in Figure 2 were obtained from interior ballistic calculations at the axial location of most severe erosion damage in tank cannon firing. Note the much higher convection coefficient during the first millisecond, a significant change from the constant value over several milliseconds used in prior modeling work.

PULSED LASER HEATING RESULTS

A Nd:YAG laser described in prior work [1,5] was used here to apply a single, uniform, circular heating pulse to the surface of each 2 mm thick, 8 mm square ceramic sample. The heating pulse diameter was 1.8 mm for SiAlON, 2.6 mm for ZrO_2, and 3.4 mm for the other materials. Two or more samples of each of the seven ceramics were heated, and the results here are from the sample whose total heat input was closest to 0.9 J/mm^2, measured by calorimetry [5]. An analysis of the laser pulse profile showed a rapid increase and slow decrease in heating during the pulse, similar to the convection coefficient plot for cannon heating in Figure 2 but longer in duration. Based on this analysis, a constant heat-input pulse of 4 ms was used to approximate laser heating in modeling discussed later.

The 4 ms, 0.9 J/mm^2 laser heating tests showed very limited damage for the three types of SiC. Only one of two SiC-2 samples cracked as in prior work [1], and none of the SiC-1 and SiC-3 samples cracked. However, all ZrO_2, Al_2O_3, Si_3N_4 and SiAlON samples cracked. Metallographic cross-sections were prepared (unetched), from which optical and scanning electron micrographs were made, as shown in Figure 3. Two general features of the cracking seem to be [i] cracks normal to the surface with consistent 0.1-0.3 mm spacing and some opening; and [ii] cracks roughly parallel to the surface and about 0.1 mm below the surface with less opening. It appears that the normal cracks are formed by the mechanism of *thermal expansion – permanent compressive deformation – tensile residual stress* discussed in prior work and here. Further, it is suggested that the parallel cracks occur after the normal cracks have formed and opened, thereby allowing tension or shear stresses to develop near the tip of an opened normal crack and to cause cracking in directions other than normal to the surface, as discussed by Evans & Hutchinson [6].

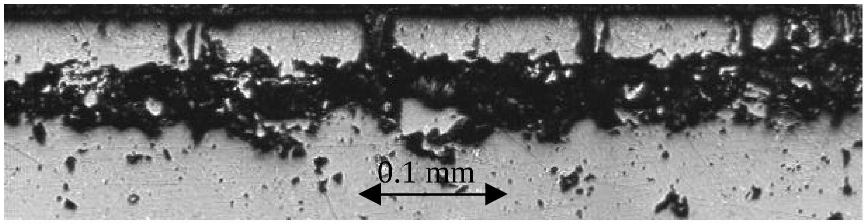

[a] Al_2O_3 (optical micrograph)

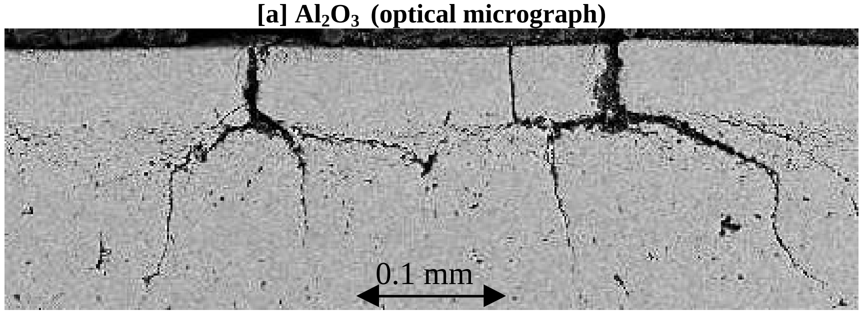

[b] ZrO_2 (scanning electron micrograph)

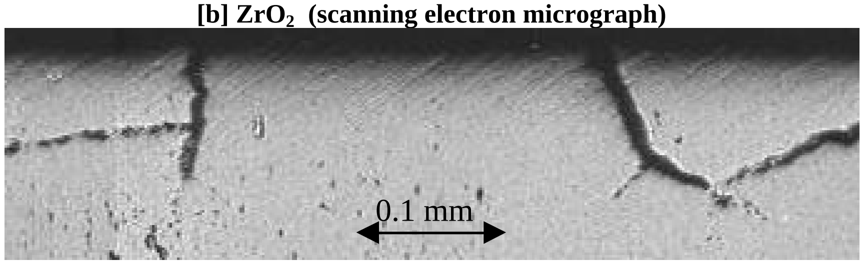

[c] Si_3N_4 (optical micrograph)

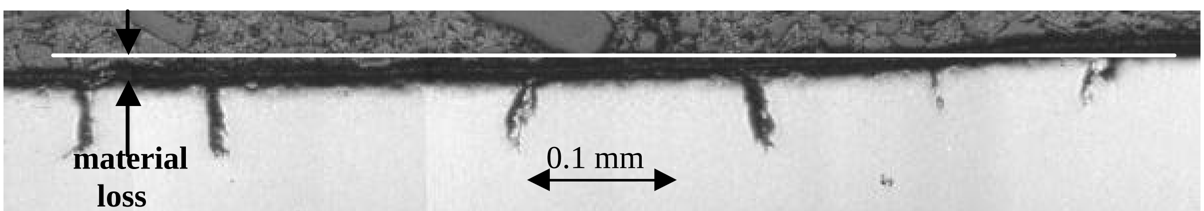

[d] SiAlON (optical micrograph)

Figure 3. Damage in four ceramics after one 4 ms laser pulse at 0.9 J.mm^2 total heat input

Some specific comments on the Figure 3 micrographs follow. The Al_2O_3 sample appears to have undergone significant fragmentation in the cracked areas, so much so that the presence of parallel cracks is much obscured. The ZrO_2 sample shows the clearest indication of normal cracks forming first and opening, followed by parallel cracks that later revert back to normal cracks. Note also the segments of surface material outlined by cracks, indicating impending fragmentation, as well as the distorted surface near the opened cracks, indicating that bending rotation may have occurred as a result of crack-face contact. The Si_3N_4 sample shows parallel cracks leading from near the tip of normal cracks, another indication that the normal cracks occurred first. The SiAlON sample shows small cracks (not easily seen in this photo) with changed direction at the tip of the normal cracks. Of more interest is the apparent loss of material in the laser-heated area of the SiAlON sample. The left edge of the photo is near the center of the 1.8 mm diameter laser "spot", and the right edge is near the outside of the spot. The line and arrows indicate a 0.02 mm loss of material, believed to be due to melting or decomposition of some constituent of the SiAlON ceramic. A general array of spherical globules was noted in the laser-heated area using a laser-scanning microscope before this sample was sectioned. None of the other six ceramics showed material loss or globules.

THERMO-MECHANICAL MODELING RESULTS

Temperature Distributions

Modeling of cannon gas heating and 0.9 J/mm^2 laser heating was performed to obtain the near-surface peak temperature distributions (and the resulting thermal stresses discussed later) for the seven ceramics and to compare the relative severity of the two heating modes. Figure 4 compares the laser and cannon heating temperatures for four of the ceramics, and Table II summarizes some of the key model results for all seven ceramics.

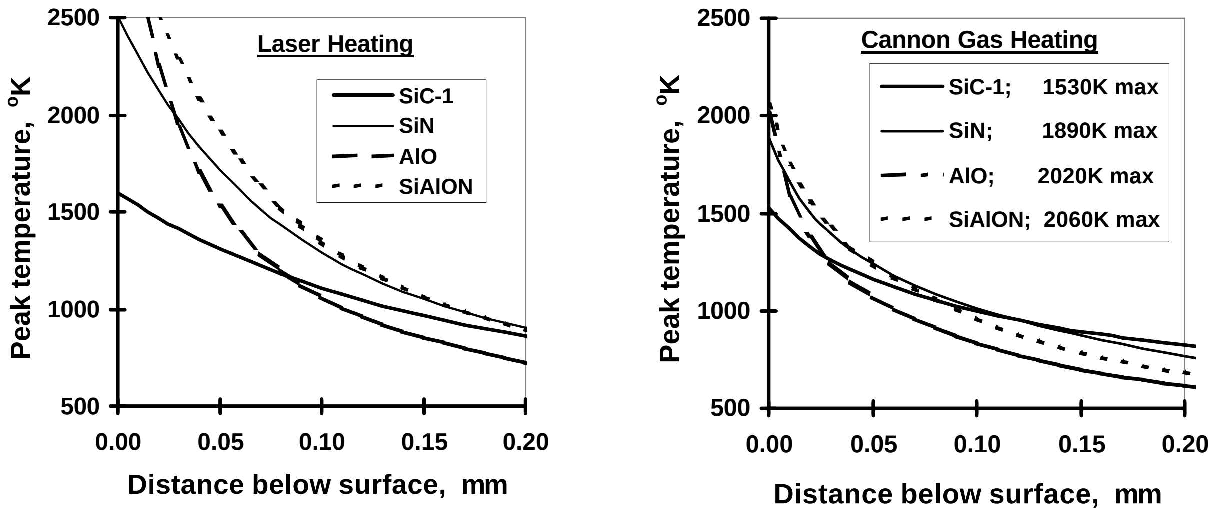

Figure 4 – Peak model temperatures for laser and cannon gas heating

Table II – Summary of model results for laser and cannon gas heating

	Conductivity, k, at 1270K W/m °K	Laser Heating; heat input, Q = 0.9 J/mm^2 T_{SURF} °K	a_{MEAS} mm	T at a_{MEAS} °K	a_{CALC} mm	Cannon Gas Heating; Fig.2 T_{SURF} °K	a_{CALC} mm	Q J/mm^2
ZrO_2	2.21	--	0.16	790	0.16	2430	0.09	0.34
Al_2O_3	7.20	3390	0.04	1710	0.13	2020	0.08	0.62
SiAlON	8.50	3070	0.04	2080	0.01	2060	**0**	0.53
Si_3N_4	14.1	2510	0.11	1230	0.01	1890	**0**	0.67
SiC-2	33.2	1710	0.04	1440	0.03	1580	0.01	0.81
SiC-1	37.3	1600	**0**	---	0.02	1530	0.01	0.84
SiC-3	45.2	1400	**0**	---	**0**	1430	**0**	0.90

As expected, the temperature distributions in Figure 4 show a rapid drop with depth. Also, some of the materials show significantly higher peak temperatures in laser heating than in cannon heating, particularly the materials with low thermal conductivity and diffusivity at high temperatures. In the laser heating model, 0.9 J/mm^2 is injected at the surface regardless of the material's thermal properties, whereas in cannon heating, materials with lower thermal conductivity and diffusivity will tend to reject heat transfer from the gas as the surface temperature goes up. It is interesting to review the surface temperatures for laser and cannon heating, shown in Figure 4 and Table II. Note that the order of surface temperatures, from high to low, is well predicted by the inverse of elevated temperature conductivity, shown in Table II for 1270 K. At the risk of over-simplicity, this indicates a "rule of thumb" that transient surface temperatures follow the inverse of elevated temperature conductivity.

Results for ZrO_2 and the other two types of SiC were not shown in Figure 4, to maintain clarity of the plots. The other SiC results were little different from those shown. The model temperatures for ZrO_2 were very high (due to low conductivity) and so far above the temperatures of available properties that the results were suspect.

Compressive Failure Predictions

The temperature distribution results, discussed above, are used to calculate the biaxial transient compressive stresses, S_T, using the following expression:

$$S_T = E\ a\ \ (T - 300\ {}^oK) / (1 - ?) \tag{2}$$

where E, a and ? are from Table I and T is the peak model temperature at a given location in the heated ceramic (plots such as Figure 4). When the transient compressive stress from Eq. 2 exceeds the elevated temperature compressive strength from Eq. 1, that is, when $S_T = S_C$, a permanent compressive displacement takes place, resulting in tensile residual stress and crack formation upon cooling.

Plots that show this model comparison of transient compressive stress with compressive strength for six of the seven ceramics are shown in Figures 5 and 6, for laser heating and cannon heating, respectively. The laser heating model results in Figure 5 predict that all ceramics except SiC-3 would crack, with crack depths approximated by the data points shown on the plots at the intersection of the compressive strength and transient compressive stress curves. These intersection points are listed in Table II as a_{CALC}. Cracking was predicted for ZrO_2, but these results were not shown, as discussed earlier in reference to Figure 4.

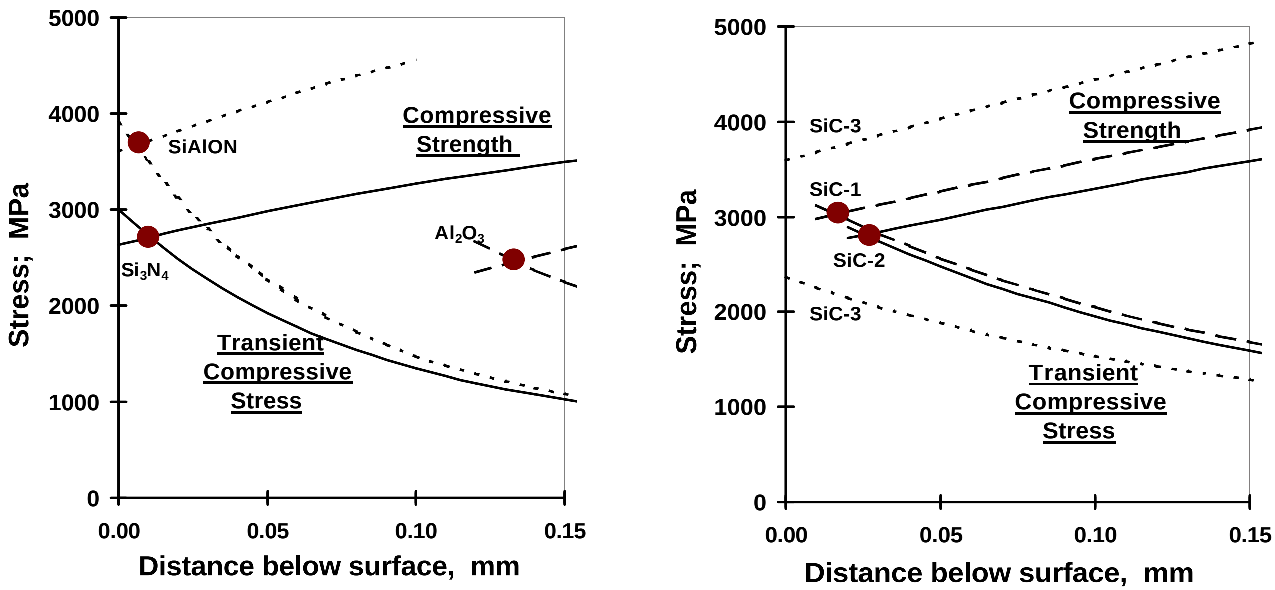

Figure 5 - Compressive failure predictions for model results from six ceramics with transient laser heating

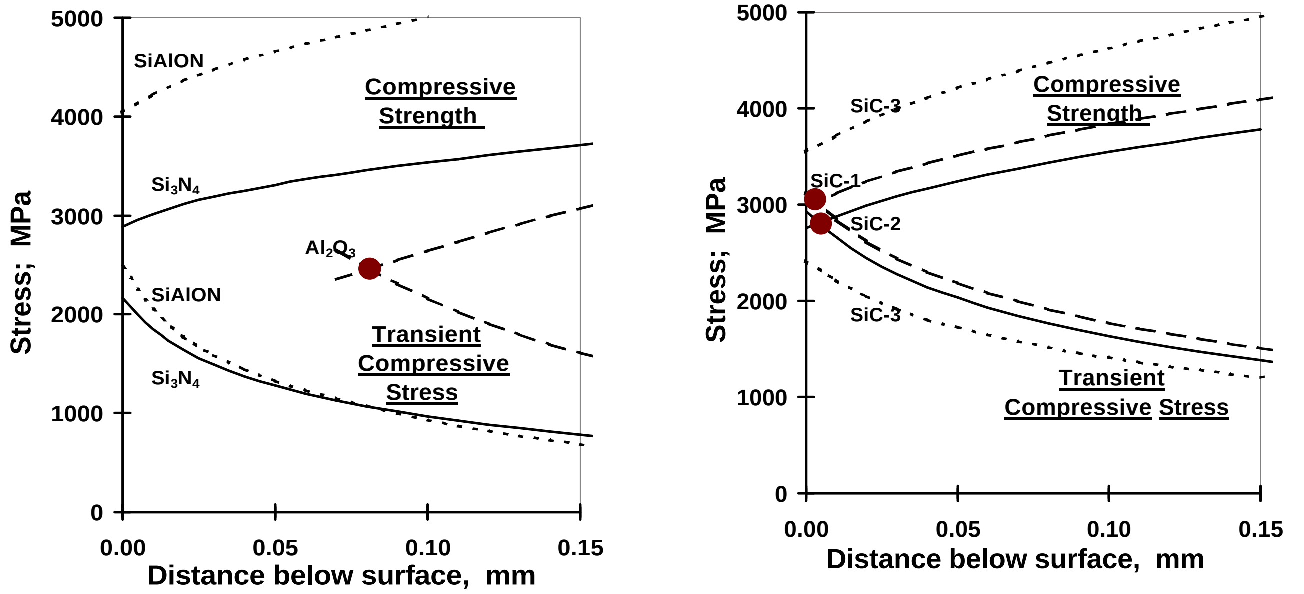

Figure 6 - Compressive failure predictions for model results from six ceramics with transient cannon heating

The cannon heating model results in Figure 6 show a marked improvement over the laser heating results, in that the predictions of crack depth (at the curve intersection points) are always at a smaller crack depth than those for laser heating. This is primarily a result of the rejection of cannon heat at high surface temperatures vs the injection of laser heat regardless of temperature, but it is also a result of the shorter heat pulse duration of cannon firing. As Table II shows, the cannon firing heat input (Q) is generally lower for materials with lower thermal conductivity at high temperature (1270K). These lower Q values indicate that the cannon heating was somewhat less severe than laser heating with Q=0.9 J/mm^2.

Finally, a ranking of suitability of the ceramics as a cannon bore thermal barrier material can be made using data from Table II. The preferred ceramics would be those with a_{CALC} = 0 and the lowest surface temperature for the cannon heating results. This rationale would rank SiC-3, Si_3N_4 and SiAlON as the most suitable; SiC-1 and SiC-2 as intermediate; and Al_2O_3 and ZrO_2 as the least suitable for a thermal barrier material under cannon bore firing conditions. This analysis and ranking of ceramics for cannon applications could be improved by additional thermal property and hot hardness data at temperatures up to those at which the damage occurs, indicated by the T at a_{MEAS} data in Table II.

SUMMARY

(i) Thermal damage modeling in ceramics was improved: by using detailed temperature-varying cannon gas temperature and convection coefficient data as input to finite difference transient temperature calculations; and by comparing compressive strength from hot hardness with near-surface compressive stress from transient heating.

(ii) Thermal damage cracks following a cannon-firing level of laser heating were observed in ZrO_2, Al_2O_3, SiAlON, Si_3N_4, and one of three types of SiC. The cracking mechanism is believed to be thermal expansion resulting in permanent compressive deformation followed by tensile residual stress and cracking upon cooling. Less damage is indicated for cannon heating because of the rejection of heat at high surface temperatures compared with the surface injection of laser heat, but also because of the shorter heat pulse of cannon firing.

(iii) Model prediction of thermal damage from typical tank cannon combustion-gas heating ranks one type of SiC as #1, Si_3N_4as #2 and SiAlON as #3, in respect to the best resistance to thermal cracks. Ranking of resistance to thermal cracks is based primarily on the ratio of transient compressive stress to compressive strength being below unity and, secondarily, on a low value of transient surface temperature.

ACKNOWLEDGEMENTS

The authors are pleased to acknowledge: the help of R. Carter and J. Swab of the Army Research Laboratory for determining thermal and mechanical properties of the ceramics; the work of L. Bell and R. Yeckley of Kennametal, Inc. for determining the elevated temperature hardness of the ceramics; and the work of S. Smith and C. Rickard of Benet Laboratories for metallographic characterization of thermal damage in the ceramics.

REFERENCES

[1] J.H.Underwood, P.J.Cote and G.N.Vigilante, "Thermo-Mechanical and Fracture Analysis of SiC in Cannon Bore Applications", *Ceramic Engineering and Science Proceedings*, **24,** 3 503-508 (2003).

[2] Laser Flash Thermal Conductivity Data supplied by Netzsch Instruments, Inc., Bedford, MA under Contract W813LT-2077-6009 with the Army Research Laboratory.

[3] N.E.Dowling, "Hardness Tests"; pp. 139-147 in *Mechanical Behavior of Materials*, 2nd ed., Prentice Hall, Upper Saddle River, NJ, pp.139-147, 1999.

[4] J.H.Underwood, A.P.Parker, G.N.Vigilante and P.J.Cote, "Thermal Damage, Cracking and Rapid Erosion of Cannon Bore Coatings", *Journal of Pressure Vessel Technology*, **125** 299-304 (2003).

[5] P.J.Cote, G.Kendall and M.E.Todaro, "Laser Pulse Heating of Gun Bore Coatings", *Surface and Coatings Technology*, **146-147** 65-69 (2001).

[6] A.G. Evans and J.W. Hutchinson, "The Thermomechanical Integrity of Thin Films and Multilayers," *Acta. Metal. mater*., **43,** 7 2507-2530 (1995).